Journal of Power Sources 205 (2012) 207–214

Contents lists available at SciVerse ScienceDirect

Journal of Power Sources

journal homepage: www.elsevier.com/locate/jpowsour

Investigation of methanol electrooxidation on Pt and Pt–Ru in H_3PO_4 using MEA with PBI–H_3PO_4 membrane

A.D. Modestov [a,*], M.R. Tarasevich [a], Hongting Pu [b]

[a] A.N. Frumkin Institute of Physical Chemistry and Electrochemistry, Russian Academy of Sciences, Leninsky Prosp. 31, Moscow 119071, Russia
[b] Institute of Functional Polymers, School of Materials Science & Engineering, Tongji University, Shanghai 201804, China

ARTICLE INFO

Article history:
Received 25 November 2011
Received in revised form 11 January 2012
Accepted 12 January 2012
Available online 21 January 2012

Keywords:
PBI
DMFC
Methanol
Electrooxidation
Pt
Pt–Ru

ABSTRACT

Electrochemical oxidation of methanol on Pt/C and Pt–Ru/C electrocatalysts was studied by slow scan rate voltammetry at 130–190 °C. The effects of partial pressures of water, methanol, and CO on the methanol electrooxidation rate were determined. It was found that methanol oxidation on Pt–Ru/C proceeds primarily via the "indirect" route through the formation of strongly adsorbed intermediate CO_{ads}, while on Pt methanol electrooxidation occurs primarily via "direct" route through the formation of weakly adsorbed intermediates. At 140 °C activity of Pt–Ru/C in methanol electrooxidation was found 2 orders of magnitude higher than that of Pt/C. Methanol oxidation reaction orders per water and methanol vapor pressures were determined. The main features of methanol electrooxidation both on Pt and Pt–Ru were accounted for assuming Langmuir–Hinshelwood mechanism of respective RDS.

1. Introduction

Current lack of infrastructure for hydrogen supply and storage makes methanol a promising fuel for fuel cells. Methanol can be produced from coal, natural gas or biomass via production of synthesis gas and its hydrogenation. Catalytic hydrogenative conversion of carbon dioxide to methanol is a way of carbon dioxide chemical recycling [1,2]. Complete oxidation of methanol in acidic electrolytes is a 6-electron reaction forming CO_2:

$$CH_3OH + H_2O = CO_2 + 6H^+ + 6e^- \quad (1)$$

Standard potential value for the methanol/oxygen fuel cell at room temperature is 1.2 V [3,4]. The spread of direct methanol fuel cells (DMFC) is hindered by sluggish methanol oxidation kinetics. Methanol oxidation mechanism is rather complex [3–13]. A simplified diagram of it is shown in Scheme 1. It consists of two different pathways [10]. A route [14–16], which leads to CO_2 through the formation of strongly adsorbed carbon monoxide, reactions (a)–(f), (i), is often called "indirect" path. This route involves four consecutive reactions of dehydrogenation, resulting in formation of adsorbed CO_{ads}, and its oxidation in Langmuir–Hinshelwood reaction (f) with adsorbed active oxygen containing species OH_{ads}:

$$CO_{ads} + OH_{ads} \rightarrow COOH_{ads} \quad (2)$$

Reaction (f) is followed by fast electrochemical reaction (i).

OH_{ads} species are formed in fast reversible water oxidation reaction [14,17]:

$$H_2O \leftrightarrow OH_{ads} + H^+ + e^- \quad (3)$$

Formation of adsorbed carbon monoxide on Pt in methanol electrooxidation was detected by various types of IR spectroscopy [12,17–27]. Characteristics of adsorbed CO layer formed on Pt electrode by oxidation of methanol were determined by radioactive labeling [28], also. Reaction (f) is considered a rate determining stage (RDS) of the methanol electrooxidation on both Pt and Pt–Ru, which proceeds by the "indirect" route. This reaction is also an RDS in electrochemical oxidation of CO on these electrodes [5,29,30].

The second "direct" reaction route leads to formation of formic acid, formaldehyde, methyl formate, methanaldimethylacetal in addition to carbon dioxide. It includes reactions (a)–(d), Lagmuir–Hinshelwood reaction (g) of intermediate species CHO_{ads} with adsorbed OH_{ads}, and fast reactions (h) and (i). All soluble compounds, which are formed in the "direct" route are omitted in Scheme 1 for simplicity. Actuality of this methanol electrooxidation route was proved by detection of formic acid, formaldehyde, methyl formate, and methanaldimethylacetal along with carbon dioxide by DEMS [31–35] and on-line mass spectrometry [9,36,37].

* Corresponding author. Tel.: +7 495 9522387; fax: +7 495 9525308.
E-mail address: modestov@elchem.ac.ru (A.D. Modestov).

0378-7753/$ – see front matter © 2012 Elsevier B.V. All rights reserved.
doi:10.1016/j.jpowsour.2012.01.089

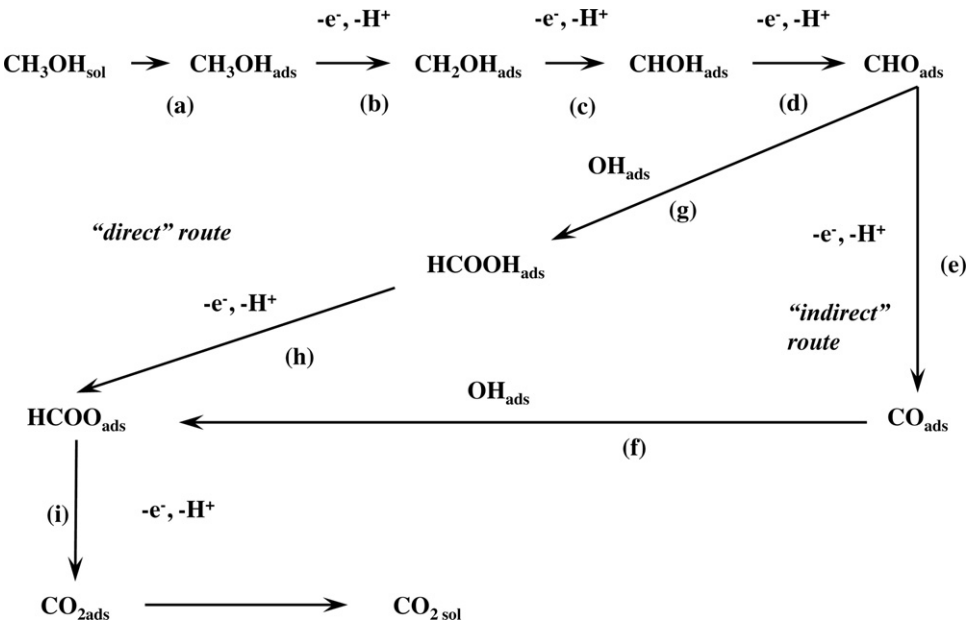

Scheme 1. Simplified representation of methanol oxidation mechanism in acidic media.

CO_{ads} is an intermediate species in methanol oxidation process, which proceeds via the "indirect" route. The route is a sequence of consecutive reactions. For this reason, the rate of the overall methanol electrooxidation process cannot exceed the rate of CO_{ads} oxidation reaction (f). However, for the methanol oxidation process, which proceeds via the second route, CO_{ads} is a poisonous species, which obstructs the catalyst surface [20]. In this case the rate of methanol oxidation can exceed the rate of CO oxidation as it happens in case of hydrogen oxidation in the presence of CO impurity.

Temperature raise increases methanol electrooxidation rate [4,38,39]. However, the use of aqueous solutions limits operational temperature of DMFC by boiling temperature of methanol-water mixture. To further increase the working temperature of DMFCs it was proposed to use concentrated phosphoric acid as electrolyte [40,41] or fuel cells with the proton conducting membrane of phosphoric acid doped polybenzimidazole (PBI–H_3PO_4) [36]. As follows from [36], provided that $P_W/P_{MeOH} \geq 1$, $T \geq 150\,^{\circ}C$, the yield of CO_2 in methanol electrooxidation in DMFC with PBI–H_3PO_4 membrane on Pt and Pt–Ru is higher than 50% and 79%, respectively, the rest being methanaldimethylacetal and methylformate. P_W and P_{MeOH} stand for partial pressures of water and methanol vapors in the feed stream, respectively. Presence of methanaldimethylacetal and methylformate in the product stream indicates that at least a fraction of methanol is oxidized in this case via a "direct" route.

In our previous work we have studied electrochemical oxidation of carbon monoxide on Pt and Pt–Ru in H_3PO_4 at temperatures ranging from 120 to 180 °C using MEA with PBI–H_3PO_4 membrane [42]. The use of this MEA in the measurements helped us determine reaction orders in respect to partial pressures of carbon monoxide (P_{CO}) and water vapors. Water and methanol are reactants, which participate in methanol electrooxidation. Knowledge of methanol oxidation rate dependence on concentration of these reactants helps establish mechanism of the process. The knowledge is also important for reaching high performance of DMFC. In aqueous electrolytes reaction orders with respect to methanol (m_{MeOH}) on Pt and Pt–Ru were found close to 0.5 [14,43–45]. Negative values of m_{MeOH} were found in [46] at low methanol oxidation overvoltage. The results of these works on methanol oxidation kinetics can hardly be extrapolated to the process of methanol oxidation in DMFC with PBI–H_3PO_4 membrane since electrolyte is virtually anhydrous in that case. The goal of this work was to study kinetics of methanol oxidation on Pt and Pt–Ru catalysts in phosphoric acid in temperature range 130–190 °C, paying special attention to dependence of methanol oxidation rate on P_W and P_{MeOH}, and to compare results with the features of CO electrooxidation kinetics established earlier under similar experimental conditions [42].

2. Experimental

MEA preparation protocol and experimental setup were described in detail elsewhere [47,48]. Briefly, MEAs of 6 cm^2 active area were used in order to match with the output of potentiostat/galvanostat PARSTAT 2273 (Princeton Applied Research). FCTS-50 (Arbin) test station was employed to prepare gas mixtures of the required composition, to control the cell temperature, and back pressure. Electrochemical measurements were conducted in a cell driven mode. Gas diffusion electrodes (GDE) were manufactured by spray coating a catalyst ink on Sigracet 10DC (SGL Group) gas diffusion layers. The catalysts used were 40% Pt on carbon support from E-TEK and Pt–Ru from Johnson-Matthey HiSPEC 10000, 60% platinum group metal (PGM) supported on carbon. Counter electrodes in all cases contained Pt catalyst. PGM loading at each GDE of the MEA was within 1 ± 0.1 mg cm^{-2} range. Therefore, current density readings related per 1 mg of PGM loading numerically coincided with the current density readings related per 1 cm^2 area of MEA. Catalyst inks were prepared using Nafion 5% solution (DuPont). Nafion was used as a binder only. Dry Nafion concentration in the catalyst layers (CL) was 3% relative to carbon support. The electrolyte in the CLs of the GDEs was phosphoric acid. The films of poly[2,2-diphenyloxide-5,5-bibenzimidazole] (PBI) were supplied by the National Innovation Company "New Energy Projects". The PBI films were doped in 85% H_3PO_4 in closed vessel at 110–130 °C for at least 70 h. For electrochemical experiments the MEA was placed in a test cell (Arbin).

Gas mixtures were prepared using gas mass flow controllers, gas mixture humidification and injection of liquid methanol into the working electrode gas transfer line (GTL). Both GTLs were

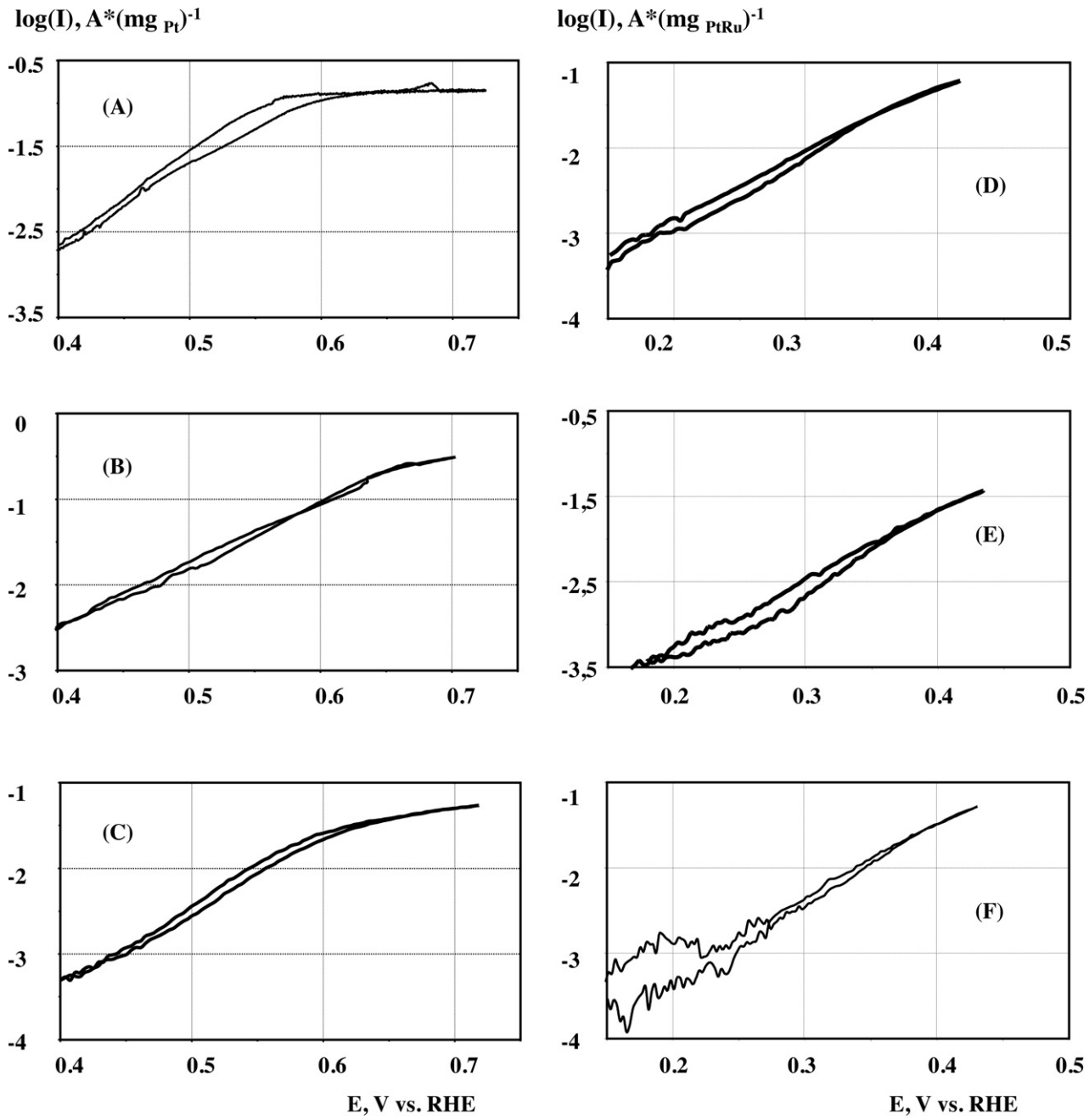

Fig. 1. Representative voltammetry curves of methanol electrooxidation on Pt (A)–(C) and PtRu (D)–(F): (A) 180 °C, P_W = 0.46 bar, P_{MeOH} = 0.024 bar; (B) 180 °C, P_W = 0.46 bar, P_{MeOH} = 0.19 bar; (C) 140 °C, P_W = 0.092 bar, P_{MeOH} = 0.046 bar; (D) 170 °C, P_W = 0.204 bar, P_{MeOH} = 0.107 bar; (E) 130 °C, P_W = 0.067 bar, P_{MeOH} = 0.041 bar; (F) 140 °C, P_W = 0.054 bar, P_{MeOH} = 0.043 bar.

kept at 120 °C. Methanol (99.8% HPLC, Sigma–Aldrich) was injected at constant rate into the GTL 15 cm apart from the cell input, where it evaporated. Syringe pump (New Era), gas tight syringe (Hamilton), and PEEK tubing were used for methanol injection. Nitrogen 99.999%, carbon monoxide 99.8%, and hydrogen 99.999% were used. Back pressure in the exhaust lines of the test cell was kept at 2 bar absolute. Composition of gas mixtures was tuned using respective gas mass flow controllers, humidification temperature, and methanol pumping rate. Concentrations of components in the gas phase are indicated in units of partial pressure (bar). Stoichiometry numbers of methanol, H_2O, and CO supply were at least 10. N_2 flow was at least 0.5 L min^{-1}. The primary role of N_2 flow was to deliver water and methanol vapors to the test cell. Counter electrode was supplied with hydrogen. Gases, which were supplied to the opposite electrodes of the MEA, were humidified to reach the same P_W. The voltammetry curves were corrected for ohmic losses. To determine cell resistance the EIS measurements were staged at open circuit voltage. 0.5 mV s^{-1} voltage scan rate was used in the voltammetry measurements. Potential of the counter electrode, which was flushed by hydrogen, under relatively low current density of our experiments almost coincides with the potential of reversible hydrogen electrode [47]. Corrections were applied to account for the Nernstian shift of the hydrogen electrode potential caused by humidification and application of the back pressure. The electrode potential readings (E) are given versus RHE.

3. Results and discussion

3.1. Methanol electrooxidation

Some representative voltammetry curves of methanol electrooxidation measured using Pt and Pt–Ru catalysts at the working electrode are shown in Fig. 1 using Tafel coordinates. The measurements were performed in the temperature range 130–190 °C. P_W and P_{MeOH} were varied in a wide range to determine dependence of methanol electrooxidation rate on partial pressures of reactants. Tafel regions on voltammetry curves with a slope ranging from 90 to 100 mV per decade on Pt–Ru and 100–140 mV per decade on Pt were observed in all cases. The regions spread over about 1.5–2 order of magnitude change of methanol oxidation current density. Deviations from Tafel type dependence were especially pronounced at high methanol oxidation overvoltage and low P_{MeOH}. Comparison of voltammetry curves shows that Pt–Ru is more active in methanol electrooxidation compared to Pt in agreement with the studies performed in aqueous electrolytes [49–55], as well as studies in concentrated phosphoric acid at elevated temperature [38,40,41]. In experiments conducted at 140 °C replacement of Pt with Pt–Ru decreased methanol oxidation overvoltage by about 0.2 V. Taking into account the slope of *I–E* curves in Tafel region of about 0.1 V per decade, this shift of voltammetry curves can be translated into about 2 order of magnitude higher activity of Pt–Ru compared to Pt.

Comparison of *I–E* curves of methanol oxidation on Pt and Pt–Ru with data on CO electrooxidation on these catalysts reported in [42] reveals that methanol and CO electrooxidation on Pt–Ru occur with comparable rates at approximately the same potentials, while on Pt methanol oxidation curves are shifted by approximately 0.1 V to less positive potentials compared to CO electrooxidation curves [42].

Fig. 2(A) shows dependence of methanol oxidation current on P_{MeOH}, which was measured on Pt catalyst at 180 °C. P_W was kept constant in this set of experiments. Current density readings were taken in the Tafel region of the respective *I–E* curves, at $E = 0.5$ V, and at high overvoltage, at which saturation of methanol oxidation current was observed, $E = 0.7$ V. Saturation of methanol oxidation current at high overvoltage was observed at $P_{MeOH} < 0.025$ bar. Respective data points measured at $E = 0.7$ V at $P_{MeOH} < 0.025$ bar are shown as solid circles in Fig. 2(A). Current density measured under these conditions was proportional to P_{MeOH}. It suggests that the process is limited by methanol mass transport in the pores of the CL. The slope of the I–P_{MeOH} dependence is about 6.6 A cm^{-2} bar^{-1}. The slope value agrees reasonably well with the slope value of the linear dependence of mass transport limited current of CO oxidation on P_{CO}, which was measured under similar conditions in [42], 6.3 A cm^{-2} bar^{-1}. In that work CO oxidation was studied using GDE containing 60% Pt–Ru with 1.4 mg cm^{-2} PGM loading. Roughly threefold increase in number of electrons per oxidized methanol molecule, compared to CO oxidation, is compensated for by more than doubling the CL thickness due to use of the catalyst with lower Pt loading in this work.

As follows from Fig. 2(A), methanol oxidation current in Tafel region of *I–E* curve, measured at $E = 0.5$ V, decreases slightly with the increase of P_{MeOH}. It implies that at $E = 0.5$ V methanol oxidation order m_{MeOH} is negative and close to zero. The similar type of methanol electrooxidation dependence on methanol concentration in aqueous solution was observed in [46]. Fig. 2(B) shows dependence of methanol electrooxidation rate on P_W at 180 °C. I values were taken $E = 0.55$ V within the Tafel region of the respective *I–E* curves. At $P_W < 0.2$ bar methanol oxidation current was found proportional to P_W, while at $P_W > 0.2$ bar the data points rather can be fitted by logarithmic dependence of methanol oxidation rate on P_W.

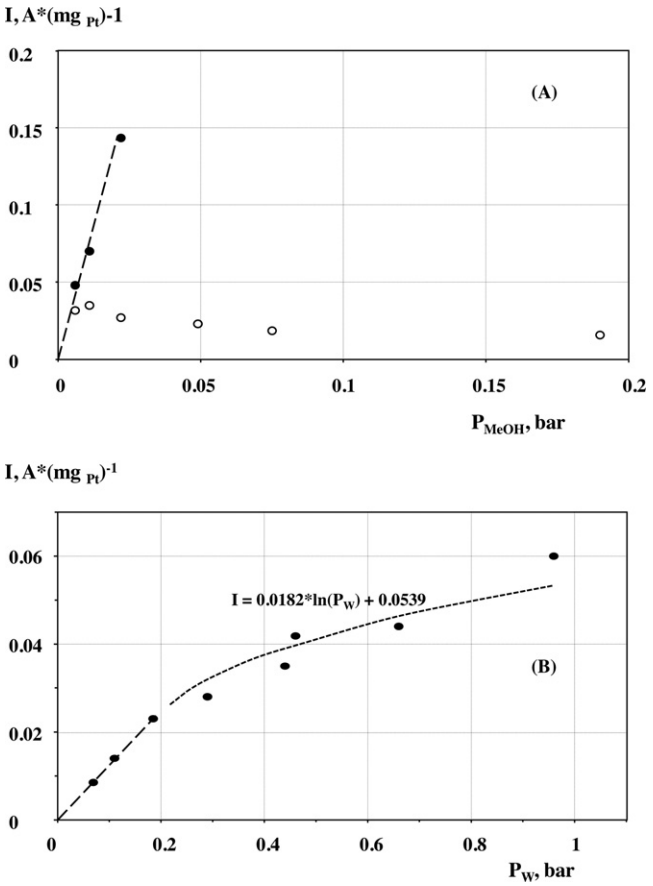

Fig. 2. Dependence of methanol oxidation current on Pt on P_{MeOH} (A) and on P_W (B) at 180 °C: (A) $P_W = 0.46$ bar, (●) limiting current at $E = 0.7$ V, (○) current at $E = 0.50$ V; (B) $P_{MeOH} = 0.075$ bar, $E = 0.55$ V.

Panels (A) and (B) in Fig. 3 show the dependence on P_{MeOH} (A) and on P_W (B) of methanol electrooxidation rate measured with Pt. Data points were sampled at 140 °C from the *I–E* curves in Tafel region. According to Fig. 3(A), at 140 °C methanol electrooxidation rate increases slightly with the increase of P_{MeOH}. The reaction order in respect to P_{MeOH}, $m_{MeOH} \sim 0.2$, was evaluated by plotting the data points in $\log(I)$–$\log(P_{MeOH})$ coordinates. According to Fig. 3(B), methanol electrooxidation rate at 140 °C increases proportionally to the increase of P_W. Therefore the respective reaction order per P_W (m_W) was close to unity.

Dependence of methanol electrooxidation rate on P_{MeOH} and P_W measured on Pt–Ru at 140 °C is shown Fig. 4, panels (A) and (B). Data points in panel (A) can be fitted as logarithmic dependence of methanol electrooxidation rate on P_{MeOH}. The reaction order averaged over the whole range of P_{MeOH} was $m_{MeOH} \sim 0.3$. Dependence of methanol electrooxidation rate on P_W is close to linear as it follows from Fig. 4(B).

The effect of temperature change on the rate of methanol electrooxidation is shown in Fig. 5. These measurements were performed under controlled water vapor and methanol vapor activity following [56]. The P_W and P_{MeOH} in the gas supply of the test cell were kept at $P_W/P_{WS} = 0.025$ and $P_{MeOH}/P_{MeOHS} = 0.005$ at all temperatures. P_W and P_{MeOH} values for these measurements were calculated using data on temperature dependence of water (P_{WS}) and methanol (P_{MeOHS}) saturated vapor pressure [57,58]. It was assumed that water and methanol molecules reach the catalyst/electrolyte interface after dissolution in electrolyte rather than directly from the gas phase. Therefore, keeping constant values of P_W/P_{WS} and P_{MeOH}/P_{MeOHS} at different temperatures keeps constant activity of water and methanol dissolved in electrolyte. Data points

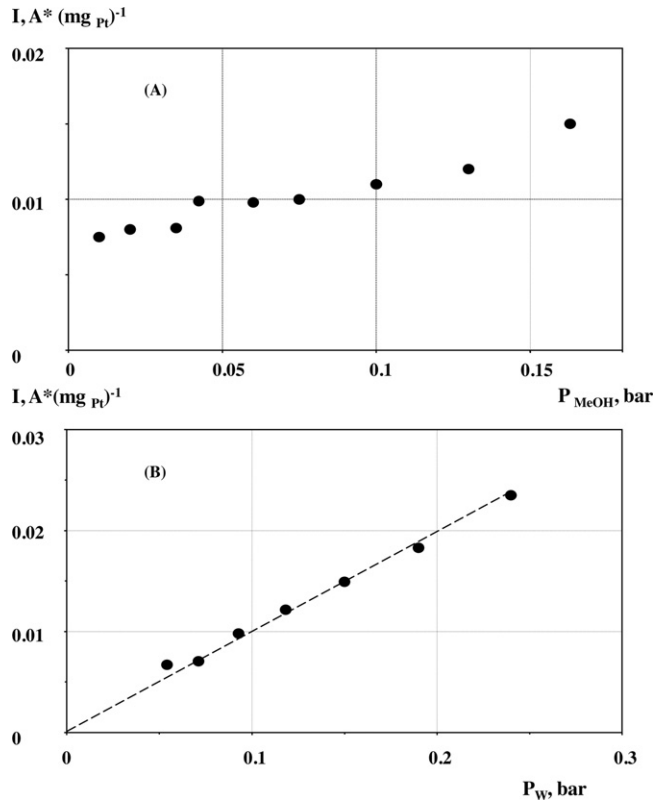

Fig. 3. Dependence of methanol oxidation current on Pt at $E = 0.55$ V on P_{MeOH} (A) and on P_W (B) at 140 °C: (A) $P_W = 0.092$ bar, (B) $P_{MeOH} = 0.043$ bar.

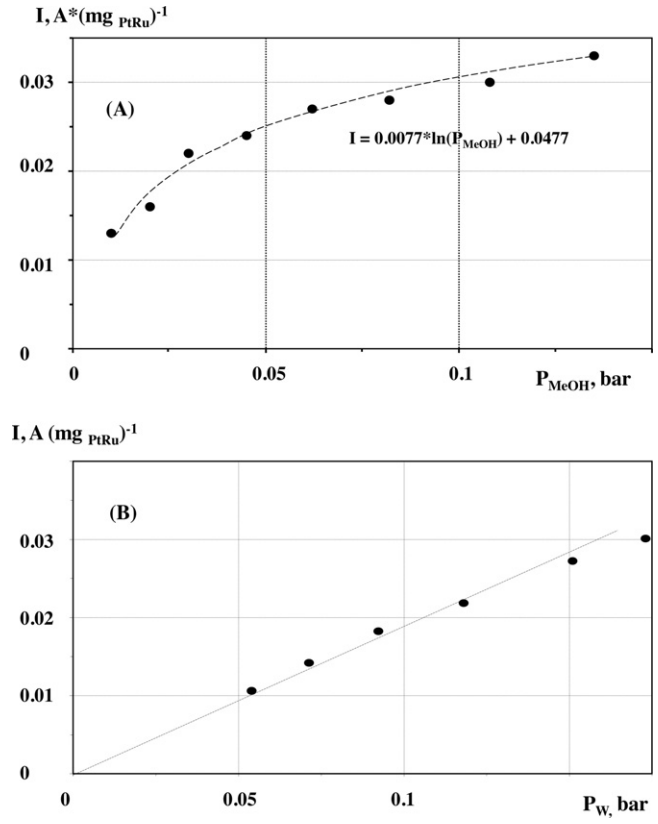

Fig. 4. Dependence of methanol oxidation current on PtRu at $E = 0.35$ V on P_{MeOH} (A) and on P_W (B) at 140 °C: (A) $P_W = 0.094$ bar, (B) $P_{MeOH} = 0.043$ bar.

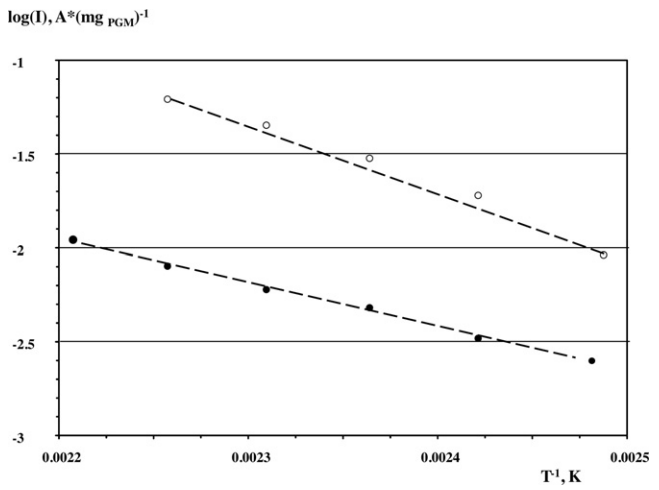

Fig. 5. Temperature dependence of MeOH oxidation current on Pt (●) at $E = 0.55$ V and on PtRu (○) at $E = 0.35$ V; P_W and P_{MeOH} were adjusted to $(P_W)/(P_{WS}) = 0.025$; $(P_{MeOH})/(P_{MeOHS}) = 0.005$ at all temperature readings.

were taken in the Tafel regions of the *I–E* curves measured on Pt and Pt–Ru at $E = 0.5$ V and $E = 0.35$ V, respectively. It is clear that the difference between the methanol electrooxidation rates on Pt and Pt–Ru increases with the increase of temperature. Apparent activation energy for methanol electrooxidation at these potentials is 44 kJ mol^{-1} and 68 kJ mol^{-1}, for Pt and Pt–Ru, respectively. Substantial difference in the values of apparent activation energy of methanol oxidation on these catalysts suggests difference in the mechanisms of methanol oxidation processes.

3.2. Methanol electrooxidation in the presence of CO in gas phase. Comparison of methanol and CO oxidation kinetics

Removal of strongly adsorbed CO_{ads} is supposed to be RDS in the methanol oxidation proceeding via the "indirect" route. Addition of CO to methanol in the supply flow in case of oxidation via "indirect" path is expected to augment slightly already high CO_{ads} coverage on the catalyst surface, thus increasing hindrance of the process. However, it will hardly change kinetics of the methanol oxidation dramatically. The main features of the processes of methanol oxidation and CO oxidation are expected to be much alike since RDS in both cases is reaction (f) in Scheme 1. If methanol oxidation proceeds via the "direct" oxidation path, strongly adsorbed CO_{ads}, which originates from the gas phase, acts as a poison. In this case, presence of CO in the supply gas is expected to block the catalyst surface thus preventing methanol oxidation. The actual blockage will depend on P_{CO} according to CO adsorption isotherm. Potential of methanol oxidation at high P_{CO} is expected to be shifted to the potential of CO oxidation.

The voltammetry curves measured on Pt and Pt–Ru in the presence of methanol, CO, and CO–methanol mixtures in the gas phase are shown in Figs. 6–8. CO electrooxidation voltammetry with the reasonable accuracy of current density values of ±25% repeat the curves measured in [42]. Fig. 6 shows *I–E* curves recorded at 140 °C on Pt–Ru in the presence of methanol at $P_{MeOH} = 0.047$ bar, panel (A); CO at different P_{CO}, curves (1) in panels (B)–(E); and CO + methanol gas mixtures, curves (2) in panels (B)–(E). $P_W = 0.094$ bar was kept constant in all these measurements. Methanol–CO mixtures were prepared with $P_{MeOH} = 0.047$ bar, while P_{CO} was varied from 0.044 bar to 0.006 bar. *I–E* curves of CO electrooxidation (1) in panels (B)–(E) demonstrate the minor decrease of CO oxidation rate with the increase of P_{CO} in agreement with the results of the earlier study [42]. At high CO oxidation overvoltage and low P_{CO} the process is impeded by mass transport in

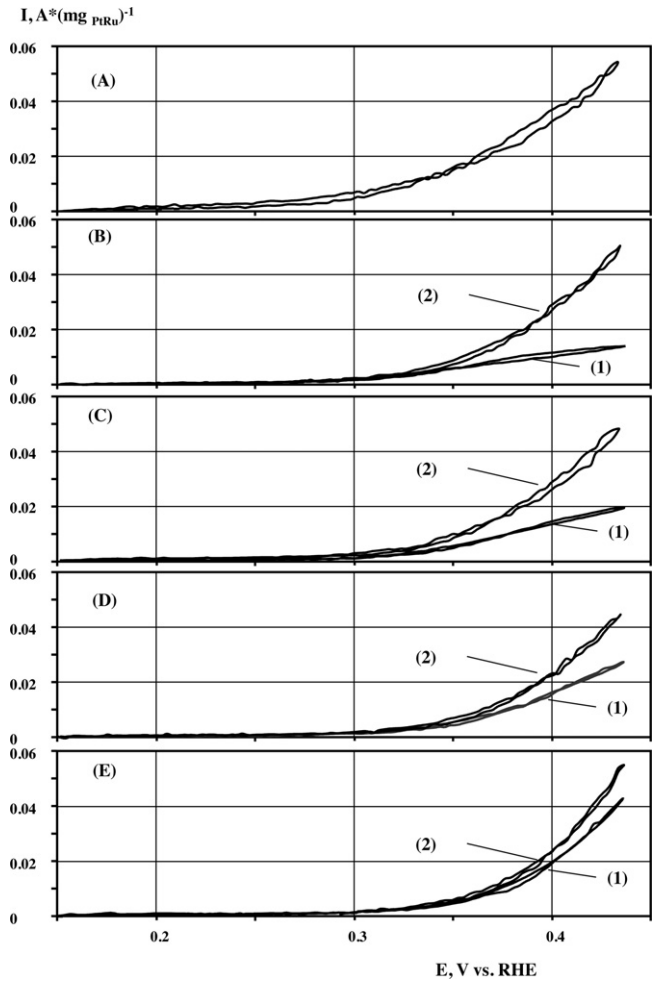

Fig. 6. Voltammetry of methanol (A), CO (1), and methanol–CO mixture (2) oxidation on Pt–Ru at 140 °C, P_W = 0.093 bar: (A) P_{MeOH} = 0.047 bar; (B) (1) – P_{CO} = 0.006 bar, (2) – P_{CO} = 0.006 bar, P_{MeOH} = 0.047 bar; (C) (1) – P_{CO} = 0.011 bar, (2) – P_{CO} = 0.011 bar, P_{MeOH} = 0.047 bar; (D) (1) – P_{CO} = 0.022 bar, (2) – P_{CO} = 0.022 bar, P_{MeOH} = 0.047 bar; (E) (1) – P_{CO} = 0.044 bar, (2) – P_{CO} = 0.044 bar, P_{MeOH} = 0.047 bar.

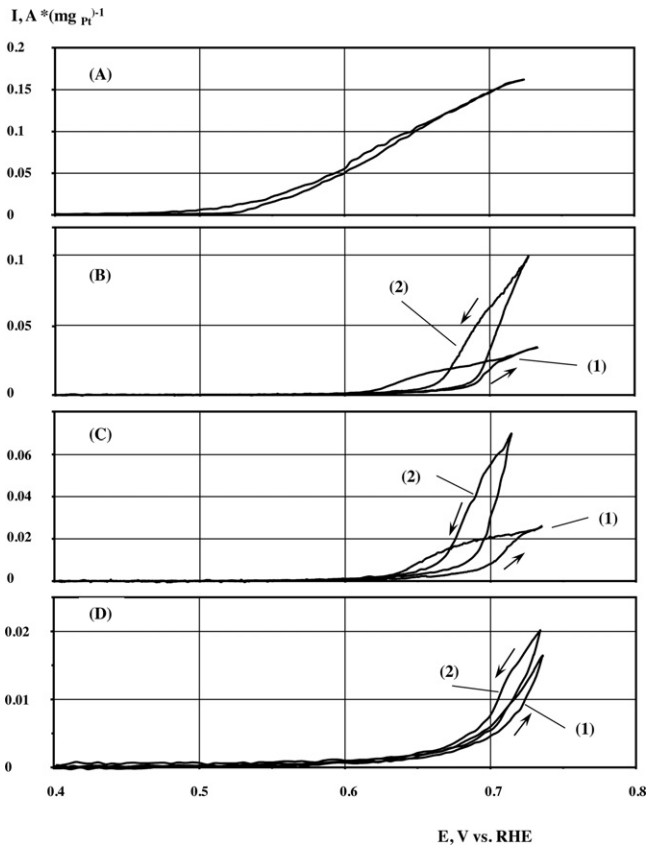

Fig. 7. Voltammetry of methanol (A), CO (1), and methanol–CO mixture (2) oxidation on Pt at 140 °C, P_W = 0.093 bar: (A) P_{MeOH} = 0.047 bar; (B) (1) – P_{CO} = 0.005 bar, (2) – P_{CO} = 0.005 bar, P_{MeOH} = 0.047 bar; (C) (1) – P_{CO} = 0.011 bar, (2) – P_{CO} = 0.011 bar, P_{MeOH} = 0.047 bar; (D) (1) – P_{CO} = 0.022 bar, (2) – P_{CO} = 0.022 bar, P_{MeOH} = 0.047 bar.

the GDE, curves (1) in panels (B) and (D). The *I–E* curves of methanol oxidation, panel (A), and CO oxidation curves (1) in panels (B)–(E), are alike. Slope of the Tafel region of methanol oxidation curve is about 100 mV per decade that is close to the slope of CO oxidation curves recorded in [42] and measured in this work, 80–90 mV per decade. At E = 0.35 V methanol oxidation current is higher than CO oxidation current by a factor of 2–3. Taking into account that complete methanol oxidation releases 3-times higher number of electrons than CO oxidation, we find that reaction rates of methanol oxidation and CO oxidation are nearly equal. It makes impossible to extract methanol oxidation contribution from the current measured when methanol–CO mixture was supplied to the electrode, curves (2) in panels (B)–(E). According to these curves anodic current slightly decreases with the increase of P_{CO} in methanol–CO mixture. All this fits well with the 'indirect' methanol oxidation route, in which CO_{ads} acts as an intermediate. Increase of P_{CO} in methanol–CO mixture in this case increases CO coverage on the catalyst surface, apparently inhibiting oxidation of both methanol and CO.

Fig. 7 shows results of the similar tests performed with Pt catalyst at 140 °C. Slope of the Tafel region of methanol oxidation *I–E* curve is about 120 mV per decade, panel (A), while the slope of CO oxidation curves is about 90 mV in agreement with [42]. Curves of methanol oxidation, panel (A), and CO oxidation, curve (1) in panel (D), are separated by a gap of approximately 0.1 V. At E = 0.6 V methanol oxidation current was $\sim 50\,mA \times (mg_{Pt})^{-1}$, panel (A), while CO oxidation current at E = 0.6 V was only $\sim 1.5\,mA \times (mg_{Pt})^{-1}$, curve (1) panel (D). Presence of CO in methanol–CO mixture at the level of P_{CO} = 0.005 bar$\sim 0.1 \times P_{MeOH}$, resulted in a dramatic decrease of methanol oxidation current. At E = 0.6 V anodic current was only $\sim 1\,mA \times (mg_{Pt})^{-1}$, curve (2) in panel (B). Curves (1) and (2) in panels (B)–(D) show that in the presence of CO in the supply flow methanol oxidation commences with the beginning of CO oxidation.

Fig. 8 shows results of experiments, which were conducted at 180 °C with Pt. Negative value of CO electrooxidation order in respect to P_{CO} (m_{CO}) is revealed by a shift of CO oxidation voltammetry curves (1) to more positive potentials with the increase of P_{CO}, panels (B)–(D). Comparison of *I–E* curves of CO oxidation, curves (1) in panels (B)–(D) with *I–E* curves (2) recorded at the same P_{CO} in methanol–CO mixtures in the supply flow shows that at the scan to more positive potentials the curves (1) and (2) virtually coincide, panels (B)–(D), as long as potential of limiting current of CO oxidation is not reached. However, on reaching this potential curves (2) did not switch to methanol oxidation curve shown in panel (A), as could be expected in case of reaching P_{CO} = 0 at the catalyst surface. Apparently, it happened because in the presence of methanol limiting current of CO oxidation was not reached. The shift of CO oxidation curves (1) to positive potentials with the increase of P_{CO} results in the corresponding shift of curves (2) recorded with methanol-CO mixtures. It suggests that CO, which was added to methanol containing supply flow, acts like a poison to methanol oxidation on Pt. On the other hand, CO_{ads}, which is

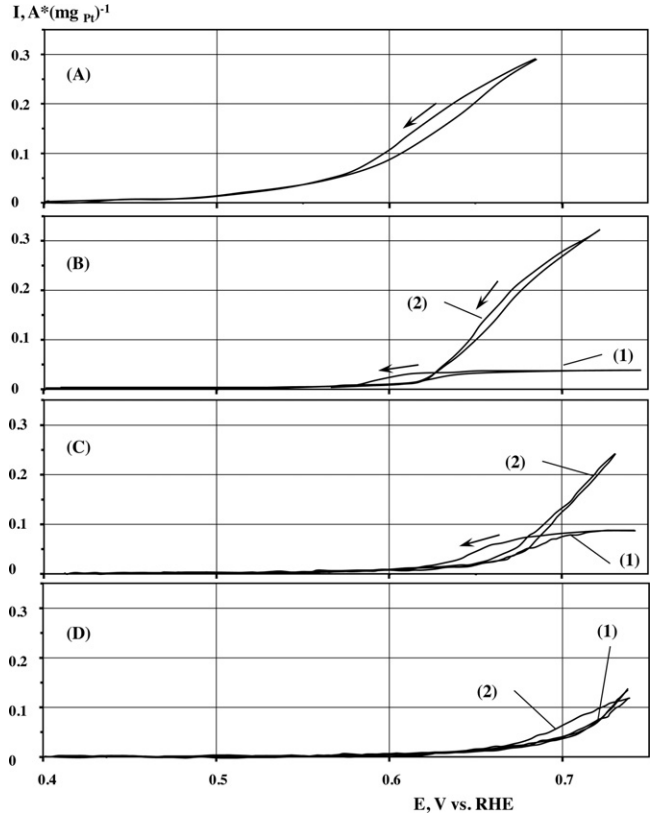

Fig. 8. Voltammetry of methanol (A), CO (1), and methanol–CO mixture (2) oxidation on Pt at 180 °C, P_W = 0.24 bar: (A) P_{MeOH} = 0.13 bar; (B) (1) – P_{CO} = 0.013 bar, (2) – P_{CO} = 0.013 bar, P_{MeOH} = 0.13 bar; (C) (1) – P_{CO} = 0.035 bar, (2) – P_{CO} = 0.035 bar, P_{MeOH} = 0.13 bar; (D) (1) – P_{CO} = 0.07 bar, (2) – P_{CO} = 0.07 bar, P_{MeOH} = 0.13 bar.

produced by methanol oxidation in a side reaction (e) (Scheme 1) increases CO_{ads} coverage impeding CO oxidation.

Results of comparative *I–E* studies of oxidation of CO, methanol and methanol–CO mixtures suggest that methanol oxidation paths on Pt and Pt–Ru under these experimental conditions differ. On Pt methanol oxidation proceeds mostly by "direct" oxidation route. On Pt–Ru the situation is opposite; the main fraction of methanol is oxidized apparently by "indirect" route. The results of MS study of exhaust gases of DMFC with PBI–H_3PO_4 membrane conducted in [36] support this conclusion. In that work the CO_2 yield increased with the use of Pt–Ru in place of Pt at the anode. For example at 160 °C, P_W/P_{CO} = 1, *E* = 0.45 V the yield of CO_2 was 83% on Pt–Ru and 56% on Pt, the rest being methanaldimethylacetal and methylformate. The exact fraction of "direct" route contribution can hardly be evaluated by MS studies, since amount of intermediate stable compounds – methyl formate, and methanaldimethylacetal, which reach the exhaust flow, depends strongly on the thickness and structure of the CL. Presence of methyl formate, and methanaldimethylacetal in exhaust produced using Pt–Ru catalyst indicates that methanol oxidation proceeds by both routes on this catalyst.

Observed dependence of methanol oxidation rate on the electrode potential, P_{MeOH} and P_W both on Pt and Pt–Ru consents with Langmuir–Hinshelwood mechanism of the RDS. In case of "direct" methanol oxidation route, the RDS is apparently reaction (g), while in case of "indirect" route, the RDS is reaction (f) (Scheme 1). Rate of methanol oxidation which proceeds via "indirect" route ($v_{indirect}$) is related to the surface coverages of CO (θ_{CO}) and OH (θ_{OH}) species:

$$v_{indirect} = k_f \theta_{CO} \times \theta_{OH} \quad (4)$$

The rate of methanol oxidation via "direct" (v_{direct}) is described by analogous equation, in which θ_{HCO} stands for HCO_{ads} surface coverage:

$$v_{direct} = k_g \theta_{HCO} \times \theta_{OH} \quad (5)$$

Here k_f and k_g stand for rate constants of reactions (f) and (g) in Scheme 1, respectively. At high methanol oxidation overpotential the θ_{HCO} and θ_{CO} are expected to become effectively independent of potential [17]. Assuming that water oxidation reaction (3) is fast and close to equilibrium, θ_{OH}, which is supposed to be low, can be expressed by Nernst equation as follows [17]:

$$\theta_{OH} = h P_W [H^+]^{-1} \exp\left[\frac{(E - E^0)F}{RT}\right], \quad (6)$$

where E^0 stands for the standard electrode potential of reaction (4), *h* is the Henry constant, which correlates water concentration in electrolyte with P_W. Tafel slope of the methanol oxidation curve by both routes is expected to be 2.303 *RT*/*F*, which equals to 82 mV per decade at 140 °C, and 90 mV per decade at 180 °C. The value agrees with the results of our *I–E* measurements of methanol oxidation on PtRu, 90–100 mV per decade. However, the slope of log(*I*)–*E* curves on Pt, 100–140 mV per decade, was higher than that expected according to Eq. (6). The slope increase apparently indicates that on Pt the rate of reaction (e) is comparable with the rate of reaction (f) (Scheme 1). It was taken into account that reactions (a)–(d), and (i) are common for both reaction routes and proceed at sufficiently high rate on Pt–Ru at lower overvoltage.

Dependence of methanol oxidation rate on P_W and P_{MeOH} can be rationalized taking into account that adsorption of OH, CO and HCO apparently follows respective Temkin isotherms [14,17,59,60]. According to the structure of the isotherm, at low surface coverage of the particular species, the coverage changes linearly with the partial pressure of the respective species, while at higher coverage, logarithmic dependence comes into effect. Linear dependence of methanol oxidation current on P_W was indeed observed on Pt and Pt–Ru at 140 °C and on Pt at 180 °C, at $P_W \leq 0.2$ bar (Fig. 2(B)). On Pt at P_W falling within the range 0.2–0.95 bar, at 180 °C the dependence of methanol oxidation current on P_W was close to logarithmic (Fig. 2(B)).

Dependence of methanol oxidation current on P_{MeOH} was close to logarithmic on Pt–Ru at 140 °C (Fig. 4(A)). However, on Pt methanol oxidation rate was nearly independent of P_{MeOH}. At 180 °C methanol oxidation rate slightly decreased with the increase of P_{MeOH}. At 140 °C reaction order per methanol averaged over the whole range of P_{MeOH} studied was $m_{MeOH} \sim 0.3$.

4. Conclusions

Electrochemical oxidation of methanol on Pt and Pt–Ru electrocatalysts was studied by slow scan rate voltammetry in concentrated H_3PO_4 in the temperature range 130–190 °C using MEA with PBI–H_3PO_4 membrane. The use of the MEA of this type enabled us to determine the effect of partial pressures of water, methanol, and CO on the methanol electrooxidation rate. Methanol oxidation *I–E* curves were compared with CO oxidation voltammetry and *I–E* curves of oxidation of methanol–CO mixtures of different compositions.

It was concluded that methanol oxidation on Pt–Ru under the experimental conditions proceeds primarily via the "indirect" route through the formation of strongly adsorbed intermediate CO_{ads}. On Pt methanol electrooxidation was deduced to occur primarily via "direct" route through the formation of weakly adsorbed intermediates. CO_{ads}, which is formed on Pt in methanol oxidation by side reaction, acts basically as a catalysts poison.

At 140 °C activity of Pt–Ru in methanol electrooxidation was found approximately 2 orders of magnitude higher than that of Pt. With the increase of temperature the difference in activity of these catalysts slightly increased. Apparent activation energy for methanol electrooxidation was found 44 kJ mol^{-1} and 68 kJ mol^{-1}, for Pt at E = 0.5 V, and for Pt–Ru at E = 0.35 V, respectively.

Value of m_{MeOH} was found fractional, dependent on the actual value of P_{MeOH}. On Pt/C at 180 °C the reaction order was negative, close zero. At 140 °C on Pt/C methanol oxidation rate slightly increased with the increase of P_{MeOH} within the range 0.01–0.163 bar. The respective reaction order was $m_{MeOH} \sim 0.2$. On Pt–Ru the rate of methanol oxidation increased linearly with the increase of $\ln(P_{MeOH})$. The reaction order on Pt–Ru averaged over the whole range of P_{MeOH} studied was $m_{MeOH} \sim 0.3$.

Methanol oxidation reaction order in respect to P_W was close to unity at low $P_W \leq 0.2$ bar both on Pt and Pt–Ru. On Pt at 180 ° at 0.2 bar < P_W <0.95 bar logarithmic dependence of reaction rate on P_W was observed.

The main features of methanol electrooxidation both on Pt and Pt–Ru can be accounted assuming Langmuir–Hinshelwood mechanism of the respective RDS.

Acknowledgment

The work was supported by the 3P Program of fundamental studies "Chemical Aspects of Power Generation" established by the Presidium of Russian Academy of Sciences.

References

[1] G.A. Olah, Angew. Chem. Int. Ed. 44 (2005) 2636–2639.
[2] G.A. Olah, A. Goeppert, G.K. Surya Prakash, J. Org. Chem. 74 (2009) 487–498.
[3] E. Gyenge, in: J. Zhang (Ed.), PEM Fuel Cell. Electrocatalysts and Catalyst Layers. Fundamentals and Applications, Springer-Verlag, London, 2008, pp. 165–287 (Chapter 4).
[4] J.L. Cohen, D.J. Volpe, H.D. Abruña, Phys. Chem. Chem. Phys. 9 (2007) 49–77.
[5] M.T.M. Koper, S.C.S. Lai, E. Herrero, in: M.T.M. Koper (Ed.), Fuel Cell Catalysis. A Surface Science Approach, John Wiley & Sons, Inc., Hoboken, NJ, 2009, pp. 159–208 (Chapter 6).
[6] M. Neurock, M. Janik, A. Wieckowski, Faraday Discuss. 140 (2008) 363–378.
[7] T. Iwasita, Electrochim. Acta 47 (2002) 3663–3674.
[8] M.R. Shivhare, R.G. Allen, K. Scott, A.J. Morris, E.B. Martin, J. Electroanal. Chem. 595 (2006) 145–151.
[9] T.H.M. Housmans, A.H. Wonders, M.T.M. Koper, J. Phys. Chem. B 110 (2006) 10021–10031.
[10] A. Capon, R. Parsons, J. Electroanal. Chem. 44 (1973) 1–7.
[11] J.-M. Léger, J. Appl. Electrochem. 31 (2001) 767–771.
[12] C. Coutanceau, S. Baranton, C. Lamy, in: P. Balbuena, V. Subramanian (Eds.), Theory and Experiment in Electrocatalysis, Modern Aspects of Electrochemistry 50, Springer Science/Business Media, LLC, 2010, pp. 397–501.
[13] U. Krewer, T. Vidakovic-Koch, L. Rihko-Struckmann, ChemPhysChem. 12 (2011) 2518–2544.
[14] V.S. Bagotzky, B.V. Yu, J. Electroanal. Chem. 12 (1967) 1323–1343.
[15] V.S. Bagotzky, Y.B. Vassiliev, O.A. Khazova, J. Electroanal. Chem. 81 (1977) 229–238.
[16] M.W. Breiter, J. Electroanal. Chem. 19 (1968) 131–136.
[17] K. Chandrasekaran, J.C.J. Wass, O'M. Bockris, J. Electrochem. Soc. 137 (1990) 518–524.
[18] Q. Fan, C. Pu, E.S. Smotkin, J. Electrochem. Soc. 143 (1996) 3053–3057.
[19] D. Kardash, J. Huang, C. Korzeniewski, Langmuir 16 (2000) 2019–2023.
[20] K. Kunimatsu, H. Hanawa, H. Uchida, M. Watanabe, J. Electroanal. Chem. 632 (2009) 109–119.
[21] L.W. Liao, S.X. Liu, Q. Tao, B. Geng, P. Zhang, C.M. Wang, Y.X. Chen, S. Ye, J. Electroanal. Chem. 650 (2011) 233–240.
[22] W.-F. Lin, J.-T. Wang, R.F. Savinel, J. Electrochem. Soc. 144 (1997) 1917–1922.
[23] S.X. Liu, L.W. Liao, Q. Tao, Y.X. Chen, S. Ye, Phys. Chem. Chem. Phys. 13 (2011) 9725–9735.
[24] I. Tkach, A. Panchenko, T. Kaz, V. Gogel, K.A. Friedrich, E. Roduner, Phys. Chem. Chem. Phys. 6 (2004) 5419–5426.
[25] T. Yajima, H. Uchida, M. Watanabe, J. Phys. Chem. B 108 (2004) 2654–2659.
[26] E. Boscheto, B.C. Batista, R.B. Lima, H. Varela, J. Electroanal. Chem. 642 (2010) 17–21.
[27] Z. Jusys, R.J. Behm, J. Phys. Chem. B 105 (2001) 10874–10883.
[28] P. Waszczuk, A. Wieckowski, P. Zelenay, S. Gottesfeld, C. Coutanceau, J.-M. Léger, C. Lamy, J. Electroanal. Chem. 511 (2001) 55–64.
[29] S.C.S. Lai, N.P. Lebedeva, T.H.M. Housmans, M.T.M. Koper, Top. Catal. 46 (2007) 320–333.
[30] E. Herrero, J.M. Feliu, Langmuir 16 (2000) 4779–4783.
[31] Z. Jusys, R.J. Behm, in: M.T.M. Koper (Ed.), A Surface Science Approach, John Wiley & Sons, Inc., Hoboken, NJ, 2009, pp. 411–464.
[32] M. Chojak-Halseid, Z. Jusys, R.J. Behm, J. Phys. Chem. C 114 (2010) 22573–22581.
[33] H. Wang, C. Wingender, H. Baltruschat, M. Lopez, M.T. Reetz, J. Electroanal. Chem. 509 (2001) 163–169.
[34] Y.E. Seidel, A. Schneider, Z. Jusys, B. Wickman, B. Kasemo, R.J. Behm, Langmuir 26 (2010) 3569–3578.
[35] G. García, J. Florez-Montãno, A. Hernandez-Creus, E. Pastora, G.A. Planes, J. Power Sources 196 (2011) 2979–2986.
[36] S. Wasmus, J.-T. Wang, R.F. Savinell, J. Electrochem. Soc. 142 (1995) 3825–3833.
[37] T. Iwasita, W. Vielstich, J. Electroanal. Chem. 201 (1986) 403–408.
[38] N. Wakabayashi, H. Uchida, M. Watanabe, Electrochem. Solid-State Lett. 5 (2002) E62–E65.
[39] J. Nordlund, G. Lindbergh, J. Electrochem. Soc. 151 (2004) A1357–A1362.
[40] M. Watanabe, Y. Genjima, K. Turumi, J. Electrochem. Soc. 144 (1997) 423–428.
[41] C. He, H.R. Kunz, J.M. Fenton, J. Electrochem. Soc. 144 (1997) 970–979.
[42] A.D. Modestov, M.R. Tarasevich, A.Y. Leykin, J. Power Sources 196 (2011) 2994–3002.
[43] A.N. Haner, P.N. Ross, J. Phys. Chem. 95 (1991) 3740–3746.
[44] A. Velãzquez-Palenzuela, F. Centellas, J.A. Garrido, C. Arias, R.M. Rodríguez, E. Brillas, P.-L. Cabot, J. Power Sources 196 (2011) 3503–3512.
[45] S.Lj. Gojković, T.R. Vidaković, D.R. Durović, Electrochim. Acta 48 (2003) 3607–3614.
[46] K. Scott, W.M. Taama, P. Argyropoulos, K. Sundmacher, J. Power Sources 83 (1999) 204–216.
[47] A.D. Modestov, M.R. Tarasevich, V.Ya. Filimonov, E.S. Davydova, Electrochim. Acta 55 (2010) 6073–6080.
[48] A.D. Modestov, M.R. Tarasevich, V.Ya. Filimonov, A.Yu. Leykin, J. Electrochem. Soc. 156 (2009) B650–B656.
[49] V.S. Entina, O.A. Petry, Elektrokhimiya 4 (1968) 481–678.
[50] O.A. Petry, Dokl. Akad. Nauk SSSR 160 (1965) 871–874.
[51] M. Watanabe, S. Motoo, J. Electroanal. Chem. 60 (1975) 267–273.
[52] K. Ledjeff, J. Ahn, D. Zylka, A. Heinzel, Ber. Bunsen-Ges. Phys. Chem 94 (1990) 1005–1008.
[53] S. Surampudi, S.R. Narayanan, E. Vamos, H. Frank, G. Halpert, A. Laconti, J. Kosek, S.G.K. Prakash, G.A. Olah, J. Power Sources 47 (1994) 377–385.
[54] H.A. Gasteiger, N. Marković, P.N. Ross Jr., E.J. Cairns, J. Phys. Chem. 97 (1993) 12020–12029.
[55] H. Hoster, T. Iwasita, H. Baumgärtner, W. Vielstich, Phys. Chem. Chem. Phys. 3 (2001) 337–346.
[56] A. Schechter, R.F. Savinell, J.S. Wainright, D. Ray, J. Electrochem. Soc. 156 (2009) B283–B290.
[57] J.A. Dean (Ed.), Lange's Handbook of Chemistry, 15th ed., McGraw-Hill, Inc., 1999 (Section 5).
[58] R.D. Goodwin, J. Phys. Chem. Refer. Data 16 (1987) 799–892.
[59] J.O'M. Bockris, A.K.N. Reddy, M. Gamboa-Aldeco, Modern Electrochemistry, 2A, 2nd ed., Kluwer Academic Publishers, New York, 2000, pp. 938–1030 (Chapter 6).
[60] M. Temkin, Zh. Fiz. Khim. 15 (1941) 296–332.